Available online at www.sciencedirect.com
SCIENCE DIRECT
International Journal of Pharmaceutics 310 (2006) 53–63
INTERNATIONAL JOURNAL OF PHARMACEUTICS
www.elsevier.com/locate/ijpharm

Enhancement of drug affinity for cell membranes by conjugation with lipoamino acids II. Experimental and computational evidence using biomembrane models☆

Rosario Pignatello[a,*], Salvatore Guccione[a], Francesco Castelli[b], Maria G. Sarpietro[b], Laura Giurato[a], Massimo Lombardo[a], Giovanni Puglisi[a], Istvan Toth[c]

[a] *Dipartimento di Scienze Farmaceutiche, Università degli Studi di Catania, Viale A. Doria, 6, I-95125 Catania, Italy*
[b] *Dipartimento di Scienze Chimiche, Università degli Studi di Catania, Viale A. Doria, 6, I-95125 Catania, Italy*
[c] *School of Molecular and Microbial Sciences and School of Pharmacy, University of Queensland, Brisbane, Australia*

Received 23 May 2005; received in revised form 31 October 2005; accepted 5 November 2005
Available online 18 January 2006

Abstract

Lipoamino acids (LAAs) are promoieties able to enhance the amphiphilicity of drugs, facilitating their interaction with cell membranes. Experimental and computational studies were carried out on two series of lipophilic amide conjugates between a model drug (tranylcypromine, TCP) and LAA or alkanoic acids containing a short, medium or long alkyl side chain (C-4 to C-16). The effects of these compounds were evaluated by monolayer surface tension analysis and differential scanning calorimetry using dimyristoylphosphatidylcholine monolayers and liposomes as biomembrane models. The experimental results were related to independent calculations to determine partition coefficient and blood–brain partitioning. The comparison of TCP–LAA conjugates with the related series of TCP alkanoyl amides confirmed that the ability to interact with the biomembrane models is not due to the mere increase of lipophilicity, but mainly to the amphipatic nature and the kind of LAA residue.

Keywords: Lipoamino acids; Tranylcypromine; Lipophilicity; Amphiphilicity; Differential scanning calorimetry (DSC); Biomembrane model; Langmuir–Blodgett film balance

1. Introduction

Enhancing the lipophilic character of drugs is a widely pursued strategy to overcome their difficulty in entering cells and/or crossing biological barriers, including the blood–brain barrier (BBB) (Jolliet-Riant and Tillement, 1999; Bodor and Buchwald, 2002; Waterhouse, 2003). Conjugation of drug molecules to lipoamino acids (LAA) has shown to increase biological uptake and intracellular concentration of drugs (Toth, 1994; Pignatello et al., 1998, 2004; Wong and Toth, 2001).

LAAs are α-amino acids containing an alkyl side chain. The length and structure of the side chain and the number of LAA residues can ultimately modulate the lipophilicity, stability and solubility of the resulting drug conjugate (Toth, 1994; Wong and Toth, 2001). LAAs combine the physico-chemical properties of both lipids and amino acids due to their amphipatic structure; LAA's linkage to drugs, apart from enhancing their lipophilicity, can also facilitate their interaction with cell membranes and penetration across absorption and biological barriers (Toth, 1994). Depending on the stability of the drug–LAA linkage, drug conjugation to LAAs can result in either bioreversible prodrugs or stable derivatives, displaying an intrinsic biological activity.

Two series of lipophilic amide derivatives of tranylcypromine (*trans*-(+)-2-phenylcyclopropanamine, TCP; Fig. 1) with LAA (**1a**–**7a**, Table 1) or linear alkanoic (fatty) acids (FA) (**1b**–**7b**, Table 2), both containing a short, a medium or a long alkyl

☆ Part of this work was communicated at the European Conference on Drug Delivery and Pharmaceutical Technology, Sevilla, May 10–12, 2004.

* Corresponding author. Tel.: +39 0957384021; fax: +39 095222239.
E-mail address: r.pignatello@unict.it (R. Pignatello).

0378-5173/$ – see front matter © 2005 Elsevier B.V. All rights reserved.
doi:10.1016/j.ijpharm.2005.11.044

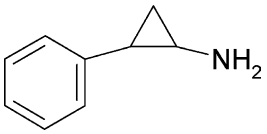

Fig. 1. Molecular structure of tranylcypromine (TCP).

Table 1
Structure and physico-chemical properties of TCP–LAA conjugates **1a**–**7a**

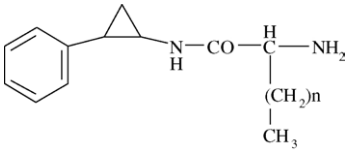

Compound	*n*	*c* log *P*[a]				*c* log $D_{7.4}$	*c* log *BB*
		A	B	C	D	B	D
1a	1	1.46	1.31	1.52	2.19	0.51	−0.2855
2a	3	2.52	2.33	2.45	3.18	1.73	−0.0762
3a	5	3.58	3.35	3.38	4.16	2.39	+0.0527
4a	7	4.46	4.37	4.30	5.14	3.52	+0.2226
5a	9	5.71	5.39	5.23	6.12	4.50	+0.3930
6a	11	7.10	7.22	6.16	7.11	6.23	+0.5994
7a	13	7.83	7.43	7.09	8.09	6.51	+0.7298
TCP[b]	–	1.21	1.37	1.59	2.41	−0.89	+0.2021

[a] Predictions were made using the following software packages: (A) ACD log *P* 5.15; (B) Pallas 3.0; (C) Osiris Property Explorer; (D) KOWIN 1.57.
[b] For TCP an experimental (*n*-octanol/water) log *P* value of 1.58 has been reported (Grunewald et al., 1984).

side chain (from 4 to 16 carbon atom chain) were previously described (Pignatello et al., 2005).

TCP is an irreversible monoamino oxidase inhibitor. In the present study, TCP was chosen as a model drug because of its simple chemical structure and low capacity to interact with phospholipid biomembrane models (personal data).

TCP–FA derivatives are characterized by an increased lipophilicity, while drug conjugation with LAAs is expected to enhance the amphiphilicity of the final compounds (Baláž, 2000). The lipophilic/amphiphilic character of TCP–LAA and TCP–FA derivatives was then assessed using computational approaches, i.e. calculation of the partition and distribution coefficients (log *P* and log *D*), as well as of the affinity to the BBB (log *BB*). Differential scanning calorimetry (DSC) and monolayer surface tension studies (Langmuir–Blodgett film balance technique) were used to check the interaction of these compounds with biomembrane models, respectively consisting of multilamellar vesicles and monolayers made of dimyristoylphosphatidylcholine (DMPC).

DSC analysis of the degree of interaction of xenobiotics, such as drugs, with this anisotropic biphasic system has already been shown to correlate with their biological behavior (Pignatello et al., 2001; Castelli et al., 2002; Saija et al., 2002; Plemper van Balen et al., 2004). Phospholipids as amphiphilic molecules form monomolecular insoluble films (called Langmuir monolayers) on the surface of a liquid. Langmuir monolayers are excellent model systems for membrane biophysics, since a biological membrane can be considered as two weakly coupled monolayers. In general, they are very useful models for studying two-dimensional ordering. Two thermodynamic variables, temperature and surface pressure, can be directly controlled (Kaganer et al., 1999). This technique was used for studying the structure and the mixing interactions of TCP–LAA with DMPC monolayers, at the air–water interface, at 37 °C and at different pressures.

Table 2
Structure and physico-chemical properties of TCP–FA amides **1b**–**7b**

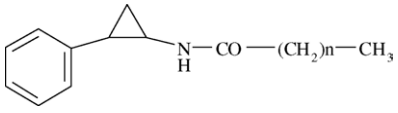

Compound	*n*	*c* log *P*[a]				*c* log *BB*
		A	B	C	D	D
1b	2	2.38	2.28	3.07	3.34	+0.2675
2b	4	3.44	3.30	4.00	4.32	+0.4747
3b	6	4.51	4.34	4.93	4.81	+0.5216
4b	8	5.57	5.36	5.86	5.73	+0.7744
5b	10	6.63	6.36	6.78	6.29	+0.9831
6b	12	7.70	7.37	7.71	7.27	+1.114
7b	14	8.76	8.39	8.64	8.25	+1.2413

[a] Predictions were made using the following software packages: (A) ACD log *P* 5.15; (B) Pallas 3.0; (C) Osiris Property Explorer; (D) KOWIN 1.57.

2. Materials and methods

2.1. Materials

TCP hydrochloride hemihydrate (Sigma) was purchased from Sigma–Aldrich Chimica S.r.l. (Milan, Italy) and was used without further purification. Compounds **1**–**7** were synthesized as described (Pignatello et al., 2005). DMPC (1,2-dimiristoyl-*sn*-glycero-3-phosphocholine C14:0) was purchased from Genzyme Pharmaceuticals (Postfach, Switzerland). All solvents were of analytical grade or higher. The water used in the study was purified by a Milli-Q UV Plus System (Millipore Corp.).

2.2. Calculation of the physico-chemical properties

The log *P* values of the synthesized conjugates were calculated using four different software packages (to validate each other and compensate for the approximation of the databases): ACD LogP 5.15 software (Advanced Chemistry Development Inc., Toronto, Canada); Pallas 3.0 (CompuDrug International, Inc. San Francisco USA); OSIRIS Property Explorer (www.actelion.com); KOWIN 1.57 [Adapted Clark method (F. Hoffmann La Roche Ltd., Basel, Switzerland)].

The distribution coefficient at pH 7.4 (apparent partition coefficient, log $D_{7.4}$) was calculated using the Pallas 3.0 software. The partition coefficient between the blood and brain (log *BB*) was calculated using the method of Clark (2001) by the KOWIN 1.57 software [Adapted Clark method (F. Hoffmann La Roche Ltd., Basel, Switzerland)] on the test compounds as .smi files. All the calculated parameters are shown in Tables 1 and 2.

2.3. Differential scanning calorimetry

MLVs were obtained by the classical thin-layer evaporation technique. DMPC or drug–DMPC mixtures at the different molar fractions (X_o = 0.01–0.09) were dissolved in 1 ml of chloroform. The solvent was evaporated off under a nitrogen flow to obtain dry thin lipid films along the vial walls. The samples were kept at 30 °C under vacuum (Büchi T-50 oven) for 6–8 h to eliminate solvent traces. The hydration of phospholipid films was made by adding 300 μl of an isotonic phosphate buffer solution (PBS, pH 7.4), to obtain a final lipid concentration of 5 mg/ml, and warming at 35 ± 2 °C for 3 min, followed by a vortex mixing for 3 min. The entire cycle was repeated three times, the suspensions were then left for a further 2 h at room temperature to reach a drug partition equilibrium between the aqueous and lipid phases.

Table 3
Experimental DSC data of DMPC liposomes containing different molar fractions (X_{DRUG}) of TCP or conjugates **1a–7a**

X_{DRUG}	T_m (°C)	ΔT%	ΔH (J/g)	$\Delta(\Delta H)$%	$T_{10\%}$–$T_{95\%}$ (°C)[a]
DMPC	24.5	–	29.1	–	24.3–26.4
TCP					
0.01	24.5	0	29.5	1.37	24.3–29.5
0.03	24.5	0	26.5	−8.93	24.3–26.2
0.06	24.4	−0.40	33.0	13.40	24.2–26.4
0.09	24.4	−0.40	26.9	−7.56	24.0–26.3
1a					
0.01	24.7	0.82	27.8	−4.46	24.4–26.6
0.03	24.6	0.41	30.9	6.18	24.3–26.1
0.06	24.5	0	32.4	11.34	24.1–26.7
0.09	24.2	−1.22	27.1	−6.87	23.7–26.5
2a					
0.01	24.5	0	22.3	−23.37	24.2–26.6
0.03	24.4	−0.41	21.4	−26.46	23.9–26.3
0.06	23.8	−2.86	28.9	−0.69	23.1–26.0
0.09	23.1	−5.71	25.1	−13.75	22.4–25.5
3a					
0.01	24.3	−0.82	27.1	−6.87	24.0–26.2
0.03	24.0	−2.04	26.5	−8.93	23.2–26.1
0.06	23.1	−4.93	22.1	−26.80	22.1–25.7
0.09	22.0	−10.20	10.0	−65.63	21.2–24.3
4a					
0.01	24.2	−1.22	25.9	−10.99	23.6–26.6
0.03	24.0	−2.04	21.3	−26.80	23.1–26.7
0.06	22.8	−6.94	19.8	−31.96	22.0–25.3
0.09	21.7	−11.43	6.09	−79.07	20.3–25.0
5a					
0.01	24.6	0.41	25.9	−10.99	24.1–26.1
0.03	24.1	−1.63	20.7	−28.87	23.1–25.8
0.06	22.6	−7.76	15.3	−47.42	21.7–26.6
0.09	21.7	−11.43	12.7	−56.36	20.2–25.3
6a					
0.01	24.5	0	23.4	−20.96	24.2–26.8
0.03	24.0	−2.04	21.6	−25.77	23.2–26.0
0.06	22.9	−6.53	14.3	−50.86	22.3–24.9
0.09	22.1	−9.79	14.3	−50.86	21.4–24.9
7a					
0.01	24.1	−1.63	24.1	−17.18	23.6–26.1
0.03	23.9	−2.45	24.0	−17.52	23.1–26.1
0.06	23.1	−5.71	10.4	−64.26	22.3–25.4
0.09	22.5	−8.16	12.1	−58.42	21.8–24.8

[a] Temperature interval from 10 to 95% of the phase transition peak.

Calorimetric experiments were performed with a Mettler DSC 12E calorimeter, connected to a Lauda Ecoline RE207 thermocryostat. The detector consisted of a chromel-constantan sensor with a thermometric sensitivity of 56 μV/°C, a calorimetric sensitivity of about 3 μV/mW, and a noise less than 60 nV (<20 μW) at 100 °C. DSC scans showed an accuracy of ±0.4 °C, with a reproducibility and resolution of 0.1 °C.

For the DSC runs, each sample was sealed in a 40 μl aluminium pan, while a pan containing 40 μl of PBS, pH 7.4 was used as the reference. Each sample was submitted to three cycles of analysis (in heating and cooling mode), at a running rate of 2 °C/min in the 5–35 °C range. A Mettler TA89A system software (version 4.0) was used to evaluate the data from each DSC run, i.e., transition peak temperature (T_m), enthalpy changes as a function of heating (ΔH), and the full width at half height of endothermal peaks ($\Delta T_{1/2}$). Further mathematical analysis was carried out on a PC using the Origin 7 SR2 software (OriginLab Corporation, Northampton, MA, USA), by which multiple peak curve fitting, subtraction of *y*-offset, and correction for time-based drift were made. Tables 3 and 4 report the obtained thermotropic data.

2.4. Permeation experiments

The time-course ability of TCP derivatives of dissolving in the aqueous phase, being absorbed onto the liposome surface and then penetrating within the inner DMPC bilayers was evaluated using two representative pairs of conjugates (compounds **2a** and **2b**, **6a** and **6b**, containing hexyl and tetradecyl side chains respectively; see Tables 1 and 2). A weighted amount of each compound was placed at the bottom of a 100-μl aluminium pan (Mettler) and covered with 80 μl of a 5 mg/ml DMPC liposome suspension, to obtain a 0.06 drug molar fraction versus DMPC. Once sealed, the pan was gently vortex mixed for 5 min, kept for 10 min at 5 °C in the calorimeter oven and then submitted to repeated heating and cooling cycles (between 5 and 35 °C), at a scan rate of 2 °C/min, separated by isothermal steps at 35 °C, to allow the migration of the drug inside the phospholipid bilayers.

2.5. Film balance measurements

A KSV minitrough apparatus was used. Phosphate buffer (pH 7.4) in ultrapure Millipore water with resistivity greater than 18.2 MΩ-cm was used as sub-phase. TCP–LAA conjugates were dissolved at a concentration of 0.3 mg/ml in chloroform. DMPC was dissolved in chloroform at a concentration of 0.7 mg/ml. Mixed DMPC/TCP–LAA solutions were successively prepared with TCP–LAA molar fractions (X_{LAA}) of 0.015, 0.03, 0.06, 0.12, 0.50, and 0.75. Drops (30 μl total volume) of the pure components (DMPC, TCP–LAA conjugates) as well of the above mixed solutions were randomly spread over the aqueous sub-phase with a microsyringe. After waiting 10 min for solvent evaporation, the floating films were linearly compressed by two mobile barriers at a rate of 5 mN/m min. Surface pressure

Table 4
Experimental DSC data of DMPC liposomes containing different molar fractions (X_{DRUG}) of TCP–FA conjugates **1b–7b**

X_{DRUG}	T_m (°C)	ΔT%	ΔH (J/g)	$\Delta(\Delta H)$%	$T_{10\%}$–$T_{95\%}$ (°C)[a]
DMPC	24.5	–	29.1	–	24.3–26.4
TCP					
0.01	24.5	0	29.5	1.37	24.3–29.5
0.03	24.5	0	26.5	−8.93	24.3–26.2
0.06	24.4	−0.40	33.0	13.40	24.2–26.4
0.09	24.4	−0.40	26.9	−7.56	24.0–26.3
1a					
0.01	24.7	0.82	27.8	−4.46	24.4–26.6
0.03	24.6	0.41	30.9	6.18	24.3–26.1
0.06	24.5	0	32.4	11.34	24.1–26.7
0.09	24.2	−1.22	27.1	−6.87	23.7–26.5
2a					
0.01	24.5	0	22.3	−23.37	24.2–26.6
0.03	24.4	−0.41	21.4	−26.46	23.9–26.3
0.06	23.8	−2.86	28.9	−0.69	23.1–26.0
0.09	23.1	−5.71	25.1	−13.75	22.4–25.5
3a					
0.01	24.3	−0.82	27.1	−6.87	24.0–26.2
0.03	24.0	−2.04	26.5	−8.93	23.2–26.1
0.06	23.1	−4.93	22.1	−26.80	22.1–25.7
0.09	22.0	−10.20	10.0	−65.63	21.2–24.3
4a					
0.01	24.2	−1.22	25.9	−10.99	23.6–26.6
0.03	24.0	−2.04	21.3	−26.80	23.1–26.7
0.06	22.8	−6.94	19.8	−31.96	22.0–25.3
0.09	21.7	−11.43	6.09	−79.07	20.3–25.0
5a					
0.01	24.6	0.41	25.9	−10.99	24.1–26.1
0.03	24.1	−1.63	20.7	−28.87	23.1–25.8
0.06	22.6	−7.76	15.3	−47.42	21.7–26.6
0.09	21.7	−11.43	12.7	−56.36	20.2–25.3
6a					
0.01	24.5	0	23.4	−20.96	24.2–26.8
0.03	24.0	−2.04	21.6	−25.77	23.2–26.0
0.06	22.9	−6.53	14.3	−50.86	22.3–24.9
0.09	22.1	−9.79	14.3	−50.86	21.4–24.9
7a					
0.01	24.1	−1.63	24.1	−17.18	23.6–26.1
0.03	23.9	−2.45	24.0	−17.52	23.1–26.1
0.06	23.1	−5.71	10.4	−64.26	22.3–25.4
0.09	22.5	−8.16	12.1	−58.42	21.8–24.8

[a] Temperature interval from 10 to 95% of the phase transition peak.

versus molecular area isotherms were recorded by film balance measurements. Before spreading the sample the sub-phase was checked for cleanliness. The experiments were performed at a sub-phase temperature of 37 °C, kept constant by a water bath. These temperature conditions were used to simulate fluid membrane behavior.

3. Results and discussion

3.1. Calorimetry studies

The main aim of this work was to establish whether the LAA moieties are able to interact to a greater extent with some biomembrane models, with respect to alkylamine residues having similar structure and lipophilicity. The partitioning into and binding of drug to cell membranes/barriers, as well as to anisotropic models such as liposomes, follow complex mechanisms and are related to the so-called 'anisotropic lipophilicity' (Plemper van Balen et al., 2004). The latter results from the hydrophobicity of the drug, as well as from its ability to make polar and ionic bonds with the membranes.

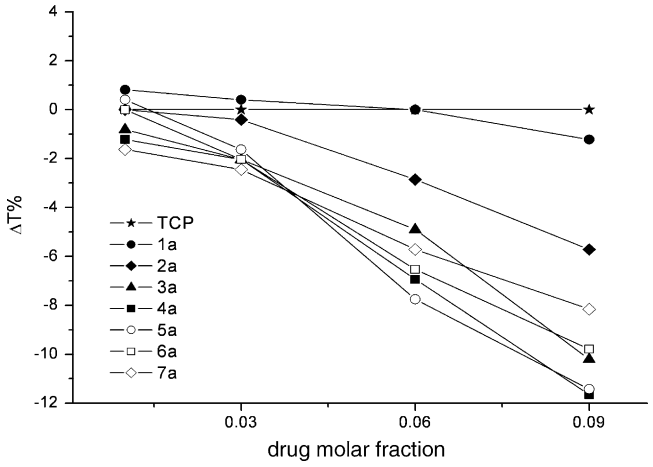

Fig. 2. Effect of increasing molar fractions of TCP–LAA conjugates on DMPC T_m value (S.D. were below ±4% and were omitted for clarity).

In our case, because of the presence of an ionizable free amine group in TCP–LAA conjugates **1a–7a** (Table 1), which is not present in the alkylamides **1b–7b** (Table 2), it is possible that polar and ionic interactions could reinforce the partitioning of TCP–LAA derivatives into DMPC bilayers, causing large changes of the various phospholipid calorimetric parameters. In Figs. 2–8 the experimental DSC data are reported, using either the changes of the main phase transition temperature in respect to pure DMPC liposomes (ΔT%) or the enthalpy changes associated to this transition [$\Delta(\Delta H)$%] as thermotropic parameters. ΔT% values were calculated as: $[(T_m - T_m^\circ) \times 100]$, where T_m° and T_m are the main transition temperature of pure DMPC and

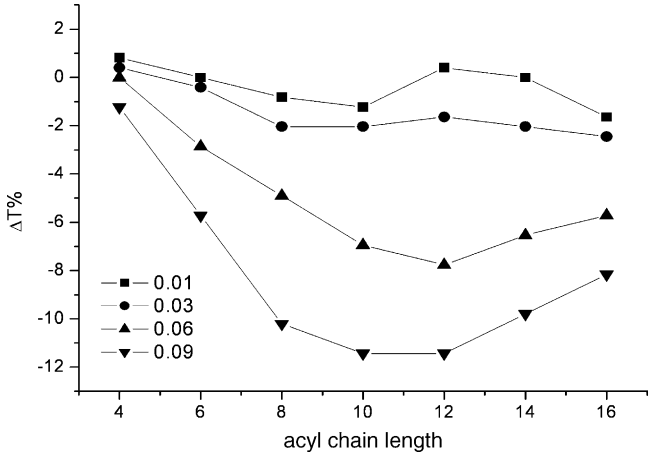

Fig. 3. Correlation between DMPC T_m variations and the acyl chain length (number of carbon atoms) for TCP–LAA conjugates **1a–7a**. The numbers in the inset indicated the drug molar fractions in the DMC liposomes.

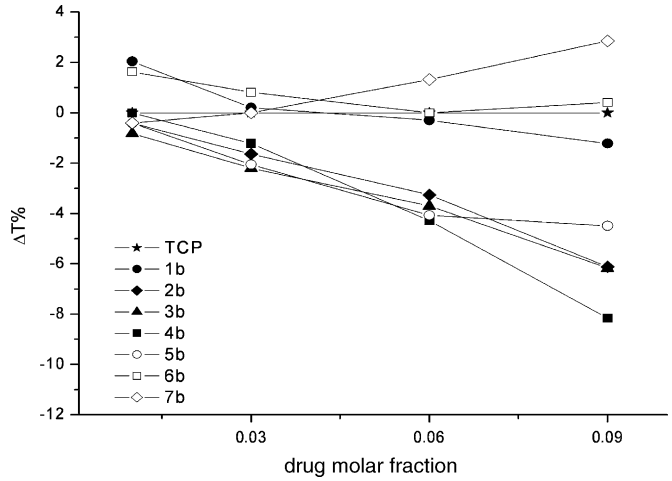

Fig. 4. Effect of increasing molar fractions of TCP–FA conjugates on DMPC T_m value (S.D. were below ±5% and were omitted for clarity).

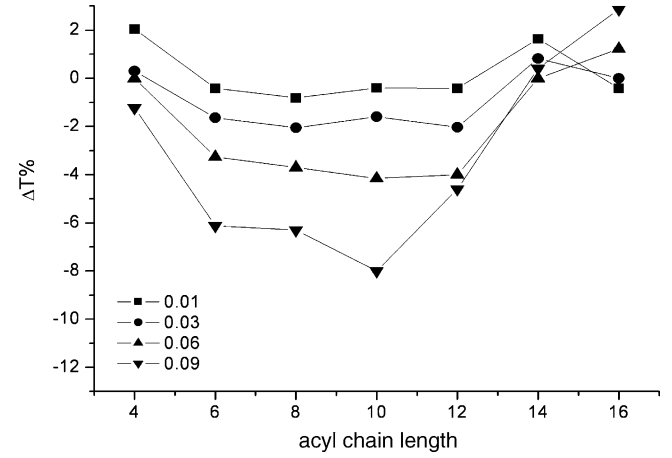

Fig. 5. Correlation between DMPC T_m variations and the acyl chain length (number of carbon atoms) for TCP–FA conjugates **1b**–**7b**. The numbers in the inset indicate the drug molar fractions in the DMC liposomes.

drug-loaded liposomes, respectively. A similar equation was used to calculate the percentage of enthalpy variations, by comparing the ΔH change of empty DMPC or drug-loaded vesicles. Both parameters were plotted as a function of the alkyl side chain

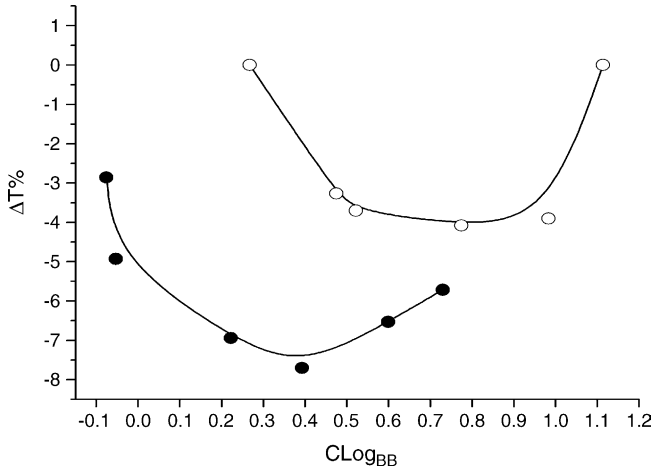

Fig. 7. Correlation between the T_m changes induced on DMPC liposomes by TCP–LAA (filled circles) or TCP–FA derivatives (open circles) as a function of the calculated log *BB* values. The six points in each curve relate to compounds **2a**–**7a** and **1b**–**6b**, respectively, whose lipophilicity (*c* log *P*) range was comparable (see Tables 1 and 2).

length (number of carbon atoms) of the LAA or alkanoic acid residue, or of the calculated log *P* value.

Increasing molar fractions of the TCP–LAA derivatives linearly affected phospholipid T_m value. The presence of pure TCP in the liposomes did not alter this thermotropic parameter, even at the highest tested drug molar fraction. Compounds **1a**–**7a** reduced the T_m value of DMPC in a concentration-dependent manner (Fig. 2).

At each drug molar fraction the T_m depression was higher with increasing lipophilicity (see compounds **1a**–**5a**) (Fig. 2). The most lipophilic derivatives **6a** and **7a** destabilized the DMPC bilayers to a lower extent than **4a** and **5a**, most probably because of their poor solubility in the aqueous medium of the liposome suspension and/or extreme lipophilicity which led to a phase separation from the phospholipid molecules, as shown by the DSC curves. The shorter alkyl chain homologue (C-4, compound **1a**) showed only marginal effects on the T_m value, indicating that its lipophilicity, even if higher than that of TCP (Table 1), is not high enough to facilitate the penetration and mixing with DMPC bilayers.

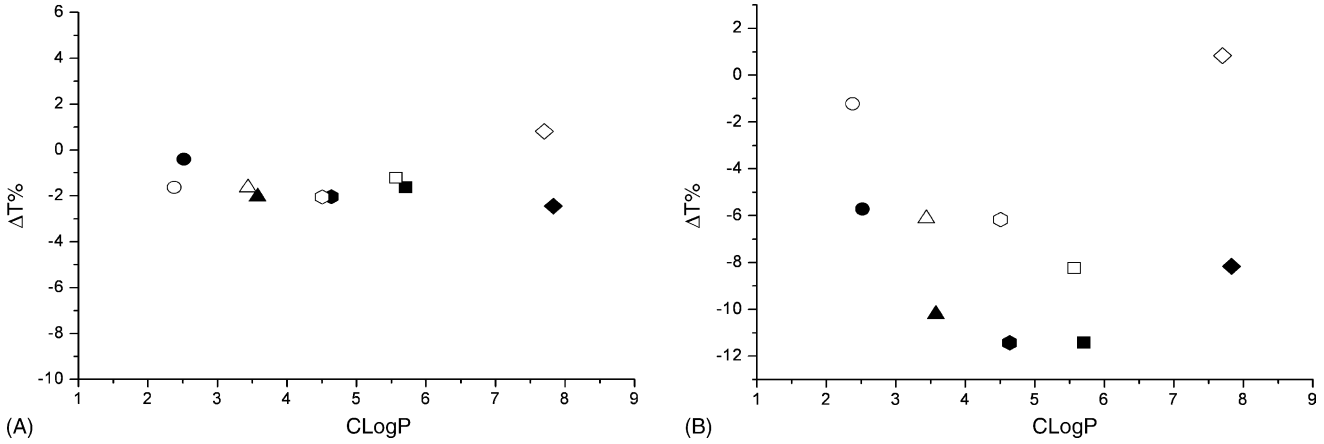

Fig. 6. DSC data (T_m changes) for selected TCP–LAA (filled symbols) and TCP–FA derivatives (open symbols), sharing similar *c* log *P* values (Panel A: molar fraction 0.03; Panel B: molar fraction: 0.09).

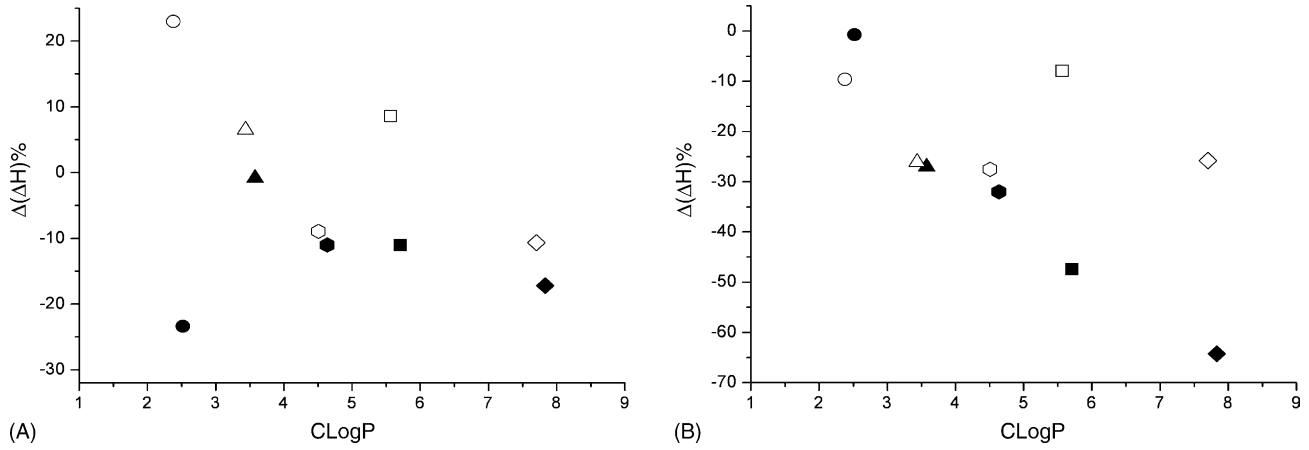

Fig. 8. Comparison between DSC data (ΔH changes) for selected pairs of TCP–LAA (filled symbols) and TCP–FA derivatives (open symbols), sharing similar $c\log P$ values (Panel A: molar fraction 0.03; Panel B: molar fraction: 0.06).

A schematic view of the relationship between the acyl chain length and ΔT% for TCP–LAA conjugates is given in Fig. 3.

At lower molar fractions the thermotropic effect on the T_m value of DMPC vesicles was similar for the entire series of conjugates. As concentration of the latter ones increased, a parabolic profile was obtained: compounds **4a** and **5a** (with a decyl and dodecyl chain, respectively) were able to strongly depress T_m, while the lower homologues (due to a reduced penetration ability into the phospholipid bilayers) as well as the higher terms of the series (because of a lower solubility in the aqueous medium) exerted only a limited effect on the vesicles.

A similar parabolic profile was observed when the ΔT% values were plotted against the calculated partition coefficient ($c\log P$) or apparent distribution coefficient at pH 7.4 ($c\log D_{7.4}$) of the conjugates (data not shown). Such a pH value was chosen for $\log D$ since it corresponds the buffer solution used for liposome preparation in the DSC experiments. All TCP–LAA conjugates have pK_a values around 8–9 (Pallas 3.0), therefore at pH 7.4 they are in a dissociated state. We used averaged partition and coefficient values for the four software packages used (Tables 1 and 2) in order to compensate for the approximation of the databases. The superimposable curves obtained suggest that the lipophilicity of the derivatives drives the observed thermotropic effects on DMPC bilayers, while the increased polarity that characterizes their dissociated form affects only marginally the interaction with the phospholipid bilayers.

In Fig. 4 the relationship between DMPC T_m changes and molar fraction of the TCP–FA derivatives **1b**–**7b** is reported. All but the lowest butyl homologue **1b** and the two terms with the longer acyl chain (the tetradecyl- and hexadecylamides **6b** and **7b**) depress the T_m value to a similar extent, although less than the corresponding TCP–LAA series (cf. Fig. 2). The higher homologues **6b** and **7b** increased the T_m value (Fig. 4), suggesting that the outermost lipophilicity hindered their mixing with phospholipids during the formation of liposomes, thus giving a negligible thermotropic interaction.

The correlation between the ΔT% and the length of the acyl chain in these compounds confirmed their reduced capacity of depressing the T_m (Fig. 5), although the same parabolic profile as above was observed. Within this series of derivatives, the decylamide **4b** exerted the maximum effect on DMPC bilayers.

To further analyze the thermotropic behavior of the two series of compounds, TCP–LAA and TCP–FA derivatives were compared by plotting the ΔT% versus $c\log P$ values (see Tables 1 and 2). For the lower drug molar fractions (0.01 and 0.03) only small differences in ΔT% were registered (Fig. 6A). The thermotropic effects of TCP–LAA and TCP–FA amides with a close lipophilicity were similar; however, the pair of compounds with the highest $\log P$ (**7a** and **6b**) showed a different behavior, the TCP–LAA conjugate being able to strongly interact with the DMPC bilayers better than the TCP–FA derivative.

On the contrary, at higher drug molar fractions the effects on the T_m were greater for the whole set of compounds (Fig. 6B). In particular, each TCP–LAA conjugate displayed greater thermotropic effects than the corresponding TCP–FA amide with a similar $\log P$. LAA conjugates then appeared more able to penetrate across DMPC bilayers and to modify their ordered packaging. A similar correlation profile was also obtained by plotting the T_m changes versus the calculated $\log BB$ values instead of the $\log P$ values (data not shown).

In Fig. 7, the correlation between T_m changes and calculated $\log BB$ is reported for the two series of compounds synthesized. For a correct comparison, both series were limited to six derivatives, not considering the least and most lipophilic compounds **1a** and **7b**, respectively, so as to keep a similar $\log P$ range (see Tables 1 and 2).

The $\log BB$ value represents a valid parameter to predict the crossing of the BBB and partition into the CNS by a drug when administered systemically. It is well known that lipophilicity is one of the most important parameters to describe the biodistribution of potential drugs. However, several independent groups have shown that surface properties as well as charge descriptors have an additionally large impact on the permeability and distribution of drug molecules. With respect to $\log P$ and in agreement with the Clark's method (2001), for the $\log BB$ calculation the lipophilic parameter is correlated to the polar surface area (PSA) of the molecule, defined as the contribution of oxygen and nitrogen atoms (as well as the bound hydrogen atoms) to

the overall molecule surface area. Although the described compounds are quite similar, their log *P* values cannot be used to describe the log *BB* values with sufficient precision, as is also evident from the different plots reported below (ΔT% versus log *P*/log *BB*, cf. Fig. 6). The r^2 values are less than 1, the best correlation obtained between log *BB* and calculated lipophilicity being 0.82 for the compounds tested.

In agreement with the published data, compounds with *c* log *BB* values greater than +0.3 are expected to efficaciously cross the BBB, whereas compounds with values lower than −1.0, which might be due to the presence of hydrogen bonding atoms, poorly distribute in brain tissue. TCP–LAA conjugates **1a**–**7a** gave a wide range of *c* log *BB* values, ranging from −0.2855 to +0.7298 (Table 1). The lower homologues **1a**–**3a** showed reduced values compared to TCP (*c* log *BB* = +0.2021), but the remaining more lipophilic terms, containing a decyl or longer side alkyl chain, showed values associated to a better prediction of crossing the BBB.

The corresponding TCP–FA amides **1b**–**7b** gave higher *c* log *BB* values than the free drug, ranging from +0.2675 to +1.2413 (Table 2). These results reflect their chemical structure (absence of the free amine group) and the consequent lower PSA values. In particular, the higher terms **5b**–**7b** gave log *BB* values close to or higher than +1.0, a threshold value above which a possible concrete difficulty of crossing the BBB and entering cells can be envisaged.

The comparison of the last three compounds with the corresponding TCP–LAA derivatives **5a**–**7a** (Table 1) confirms that the LAA groups modulate the lipophilicity/amphiphilicity of the drug molecule, avoiding extreme log *BB* values even for compounds with a very high *c* log *P* (up to 8.0). More specifically, Fig. 7 clearly shows that the entire series of TCP–LAA conjugates (dotted circles), which displayed lower *c* log *BB* values, exerted deeper effects on DMPC bilayer organization than the corresponding series of TCP–FA amides (open circles). For instance, the hexyl and octyl homologues **2a** and **3a** gave a T_m depression comparable to the much more lipophilic terms of the TCP–FA series **2b**–**5b**. The strongest effects on DMPC T_m were given by TCP–LAA conjugates with a *c* log *BB* value between 0.2 and 0.6. However, the FA amides with similar *c* log *BB* values were less able to alter the phospholipid phase transition temperature.

As discussed above, log *BB* is considered a more reliable and complete parameter than log *P* to predict the capacity of a drug to cross the BBB (Clark, 2001). On the other hand, phospholipid vesicles are often used as a suitable 3D model for studying the effects of drugs on cell membranes and to obtain valid structure–activity relationships (Baláž, 2000; Pignatello et al., 2001; Castelli et al., 2002; Saija et al., 2002; Plemper van Balen et al., 2004). Our DSC data however suggest that this experimental model is rather incomplete to correlate the thermotropic effects of the tested compounds on DMPC bilayers with their calculated log *BB* values, at least as compared with *c* log *P* ones.

The effects on the enthalpy changes associated with the DMPC main transition phase (ΔH) were less linear than those exerted on T_m values. TCP–LAA conjugates **1a**–**7a** caused a progressive broadening of the endothermic peak associated to the DMPC phase transition, with a simultaneous reduction of the ΔH value (Table 3). This is particularly evident for the 0.06 and 0.09 drug molar fractions; for the higher homologues an incipient phase segregation and loss of co-operativity in the phospholipid bilayers was also observed (not shown). These findings suggested that the TCP–LAA conjugates (at least those with an intermediate lipophilicity and solubility) are able to mix with the DMPC molecules, altering their packing and geometry.

TCP–FA amides **1b**–**7b** showed a progressive reduction of ΔH with increasing molar fraction, but to a much reduced extent than the corresponding TCP–LAA conjugates (Table 4). Starting from the dodecyl-amide **5b** phase segregation signs were clearly visible in the DSC curves, even at low molar fractions (not shown). The enthalpy changes are mainly due to non-polar interactions between the host drug and the acyl phospholipids chains. The calorimetric results indicate that the TCP–FA amides are able to penetrate into DMPC bilayers only at low concentrations. Higher drug molar fractions led to precipitation/segregation inside the bilayers, reducing the changes exerted on DMPC thermotropic parameters.

The comparison among paired TCP–LAA and TCP–FA derivatives is reported in Fig. 8 for two drug molar fractions. These compounds gave less linear effects upon ΔH than those discussed above for T_m. At the highest tested molar fraction (0.09) the graphical analysis was not possible due the deformation of the phase transition peaks. Most TCP–FA amides showed a reduced effect upon the enthalpy changes. Less negative or positive $\Delta(\Delta H)$% values, as reported in Fig. 8, indicate a greater phase transition peak area of the vesicles prepared in the presence of the drugs. This can be due to the phase segregation of the compounds from DMPC molecules, but also to a stabilizing and packing effect of these lipid amides on the phospholipid bilayers.

The effects on the ΔH by TCP–LAA and TCP–FA pairs of derivatives, comparison based on their *c* log *P* values, become more diversified at the highest molar fraction tested (0.06, Fig. 8B). Over a certain degree of lipophilicity, i.e. a *c* log *P* greater than 5.5 corresponding to a C-12–C-14 acyl chain, the effects on ΔH were greater for TCP–LAA conjugates than for TCP–FA ones (Fig. 8B). As discussed, these results confirm that for the more lipophilic compounds, the presence of the LAA moiety (series a) promotes a deeper interaction with the biomembrane model that is better than a simple acyl chain (compounds of series b). On the contrary, at lower drug molar fractions such differences between the lipophilicity and amphiphilicity of compounds were less evident, giving a reduced magnitude of the thermotropic effects on DMPC bilayers (Fig. 8A).

3.2. Kinetic calorimetric experiments

Some TCP–LAA conjugates were incubated with preformed DMPC MLVs. Amounts of each conjugate and DMPC was chosen so as to achieve a final drug molar fraction of 0.06 in the case of a complete mixing with the phospholipids. DSC scans (in heating mode) were run after 10 min and then at 1, 2, 4, 6, 8, and 24 h, spaced by isothermal phases at 35 °C. In these experiments the amount of drug dissolved in the aqueous phase

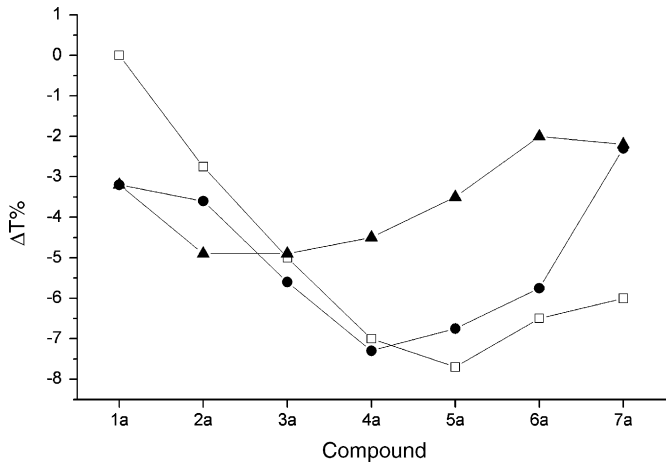

Fig. 9. Comparison of the effects exerted by TCP–LAA conjugates on DMPC T_m value during the kinetic experiments ['plateau' measured at 1–2 h (▲) or T_m change registered after 24 h (●)] with the calorimetric results observed for DMPC liposomes loaded with a 0.06 molar fraction of each conjugate (□) (cf. Table 3).

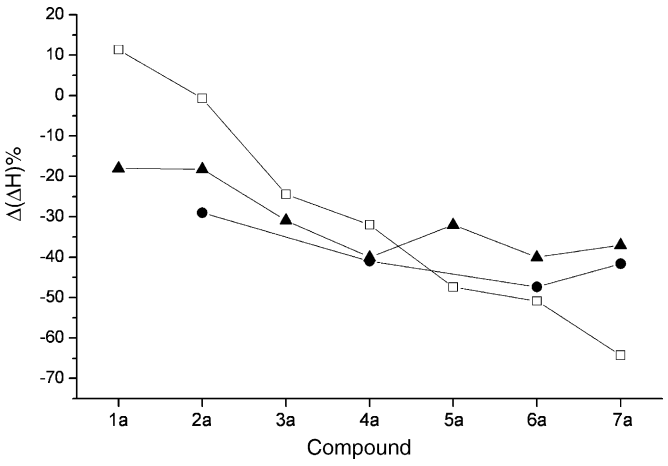

Fig. 10. Comparison of the ΔH changes registered for TCP–LAA conjugates during the kinetic experiments ['plateau' effect measured at 1–2 h (▲) or T_m change measured after 24 h (●)] with the calorimetric results observed for DMPC liposomes loaded with a 0.06 molar fraction of each conjugate (□) (cf. Table 3).

can progressively enter into contact with the superficial and then deeper phospholipid bilayers. The possible changes of the thermotropic parameters of DMPC vesicles can thus be related to the amount of drug which penetrates the bilayers over time, as well as to its localization inside the vesicles (Castelli et al., 2005). In the case of a complete miscibility of the drug with the liposomes, a DSC profile would be registered similar to that obtained when the vesicles were formed in the presence of the same 0.06 molar fraction of the drug (organic phase preparation).

Upon incubation at 35 °C, TCP–LAA conjugates exerted a quick effect on the T_m value of DMPC bilayers (Fig. 9). After approximately 1–2 h of incubation, T_m changes reached a constant value, lower than that measured when the liposomes were prepared in the organic phase with a 0.06 molar fraction of the same conjugates (Table 3). Only a portion of the incubated conjugates was able to mix with the vesicles, entering and altering the bilayer order.

The inverse correlation of this behavior with the conjugate lipophilicity can be explained in terms of a lower solubility of the higher homologues in the aqueous dispersing phase: the lack of complete solubility, would reduce their interaction with liposomes and the following mixing with the phospholipids.

Once the partition equilibrium between the aqueous medium and bilayers was achieved (after 24 h of incubation), the majority of conjugates accomplished a similar T_m depression value, close to the one measured for liposomes prepared in the presence of the same conjugates. Only the lowest (C-4) and highest homologues (C-16) showed a different behavior. These findings suggest that, by incubation at 35 °C, all the drug molecules penetrated the DMPC bilayers (or, at least, the same amount able to penetrate when the liposomes were prepared in organic phase), further outlining the ability of these conjugates to permeate the biomembrane model used in our experiments.

The effect of enthalpy changes (ΔH) was substantially quick and stable up to 24 h of incubation, with values close to those registered when the conjugates were entrapped in liposomes. Also in this case the first and last terms of the series (compounds **1a**, **2a**, and **7a**) gave a ΔH reduction respectively higher and lower with respect to what was observed with the liposomes prepared in the organic phase. These data suggest that the less liposoluble terms were able to spontaneously penetrate better into DMPC bilayers, whereas the most lipophilic term **7a** was not able to distribute easily among the bilayers and the external aqueous phase. The comparison between the ΔH changes observed in the previous experiments and those collected during the kinetic tests are reported in Fig. 10.

3.3. Langmuir–Blodgett experiments

The interactions occurring within a monolayer at the air–water interface between selected TCP–LAA conjugates (compounds **2a**, **4a**, and **6a**) and DMPC at 37 °C were examined. The isotherms of pressure as a function of the area of pure compounds as well as TCP–LAA/DMPC mixtures at different molar fractions of the conjugate are shown in Fig. 11. At this temperature, which is above the DMPC melting transition temperature (Albrecht et al., 1978), DMPC monolayers behave as a fluid membrane along all the compression isotherms curves. The pure monolayer formed by compound **2a** did not exhibit a lateral surface pressure of >4 mN/m, indicating a low surface activity at the air–water interface. The 0.015 and 0.06 molar fractions of **2a** did not affect the shape and the area per molecule of the isotherms; a 0.03 molar fraction of **2a** shifted the isotherm to higher areas per molecule, whereas higher molar fractions shifted the isotherm toward smaller areas per molecule (Fig. 11A).

The behavior of compound **4a** was different (Fig. 11B): it was in fact able to form a layer due to the longer chain allowing the packing and compression of the molecules, reaching a value of 22 mN/m upon compression. The mixture isotherms were shifted toward higher values of area per molecule up to a 0.12 molar fraction and toward lower values of area per molecule for higher molar fractions. Finally, pure **6a** isotherms showed three

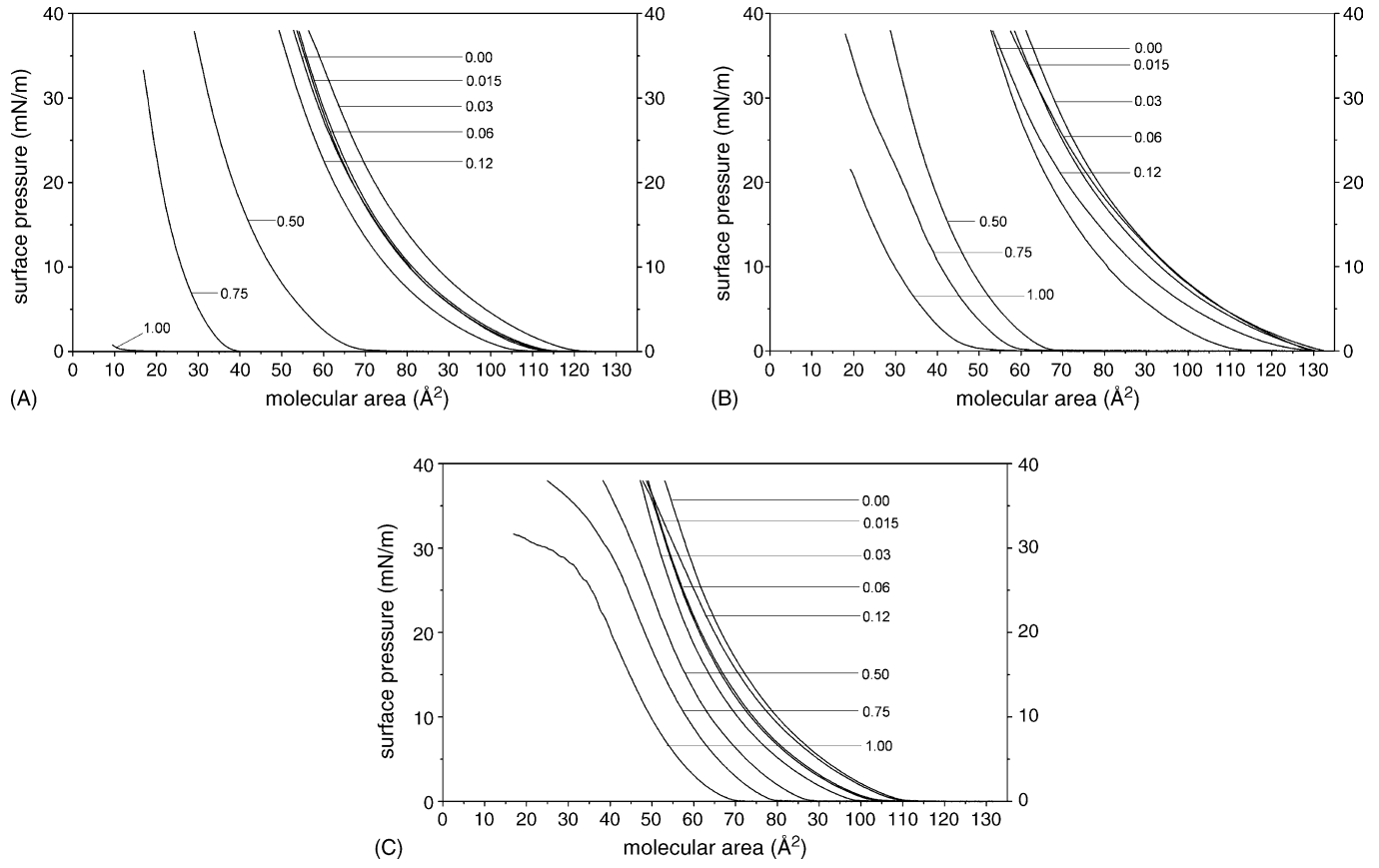

Fig. 11. Surface pressure vs. molecular area isotherms, at 37 °C, of monolayers of DMPC mixtures with TCP–LAA conjugates: DMPC/**2a** (A), DMPC/**4a** (B), and DMPC/**6a** (C). The TCP–LAA molar fraction is reported in the figure for each curve. The curves at $X_o = 0$ and 1 relate to pure DMPC and pure conjugates, respectively. S.D. values were within ±4%.

distinct regions: in the first region (130–70 molecular area) the pressure was unaffected by the barrier movement, indicating that the molecules are dispersed on the sub-phase in a gas-like phase. In the second region (∼70 to ∼35 molecular area) the pressure increase was indicative of an expanded liquid phase, where the molecules are loosely packed and still have a random orientation; the third region (35–16 molecular area) showed a liquid expanded–liquid condensed transition (Fig. 11C).

The nature and relative strength of the interactions between the two kinds of molecules can be better understood by plotting the experimental average molecular area A_{exp} versus the TCP–LAA molar fractions at a given pressure (10 or 20 mN/m). Indeed, for an ideal interaction or for completely immiscible molecules the average molecular area A_i of the mixed monolayer will be given by the expression:

$$A_i = X_{DMPC}\, A_{DMPC} + X_{TCP-LAA}\, A_{TCP-LAA}$$

where X_{DMPC} and $X_{TCP-LAA}$ are the molar fractions of the two components in the mixture, while A_{DMPC} and $A_{TCP-LAA}$ represent the average molecular areas of the pure components (Albrecht et al., 1978). A positive deviation (i.e., A_{exp} exceeding A_i) will indicate a less dense packing, while a higher film density will be revealed by a negative deviation ($A_{exp} < A_i$).

Plots of A_{exp} versus $X_{TCP-LAA}$ obtained at 10 and 20 mN/m pressures are shown in Fig. 12A. Positive deviation with respect to the ideal mixture case was clearly observed along all the studied compositional range for the conjugate **2a**, suggesting a reduced density of the formed films (Fig. 12A). With regard to DMPC/**4a** mixtures (Fig. 12B), a positive deviation for lower molar fractions was clearly visible, whereas the values obtained for higher molar fractions overlap the dotted line indicating an ideal interaction between DMPC and **4a**. The effect exerted by **6a** on the DMPC monolayer was quite different. Mixtures containing low molar fractions of **6a** showed a negative deviation, suggesting a higher film density with respect to the ideal one, while mixtures containing 0.12, 0.5, or 0.75 molar fractions showed an insignificant deviation from the ideal behavior (Fig. 12C). These results indicate that at these molar fractions, **6a** interacts ideally with DMPC. Nevertheless, **6a** could be completely immiscible with DMPC; in fact, the properties of a monolayer in which two components are immiscible will reflect those of the two component films and the area occupied by the combined film will be the sum of the areas of the separate films (Kaganer et al., 1999).

The interaction of compounds **2a**, **4a** and **6a** in the DMPC bilayers seems to be governed by different mechanisms. The molecules of **2a** are located in such a way as to allow the amino acid moiety to stay in contact with the sub-phase, and the expanding effect of **2a** on the DMPC monolayer can be due to the lower **2a**/DMPC with respect to DMPC/DMPC interactions. In fact, the short hydrophobic chain in **2a** gives only a small contribution to the hydrophobic interactions. In the case of **4a**/DMPC

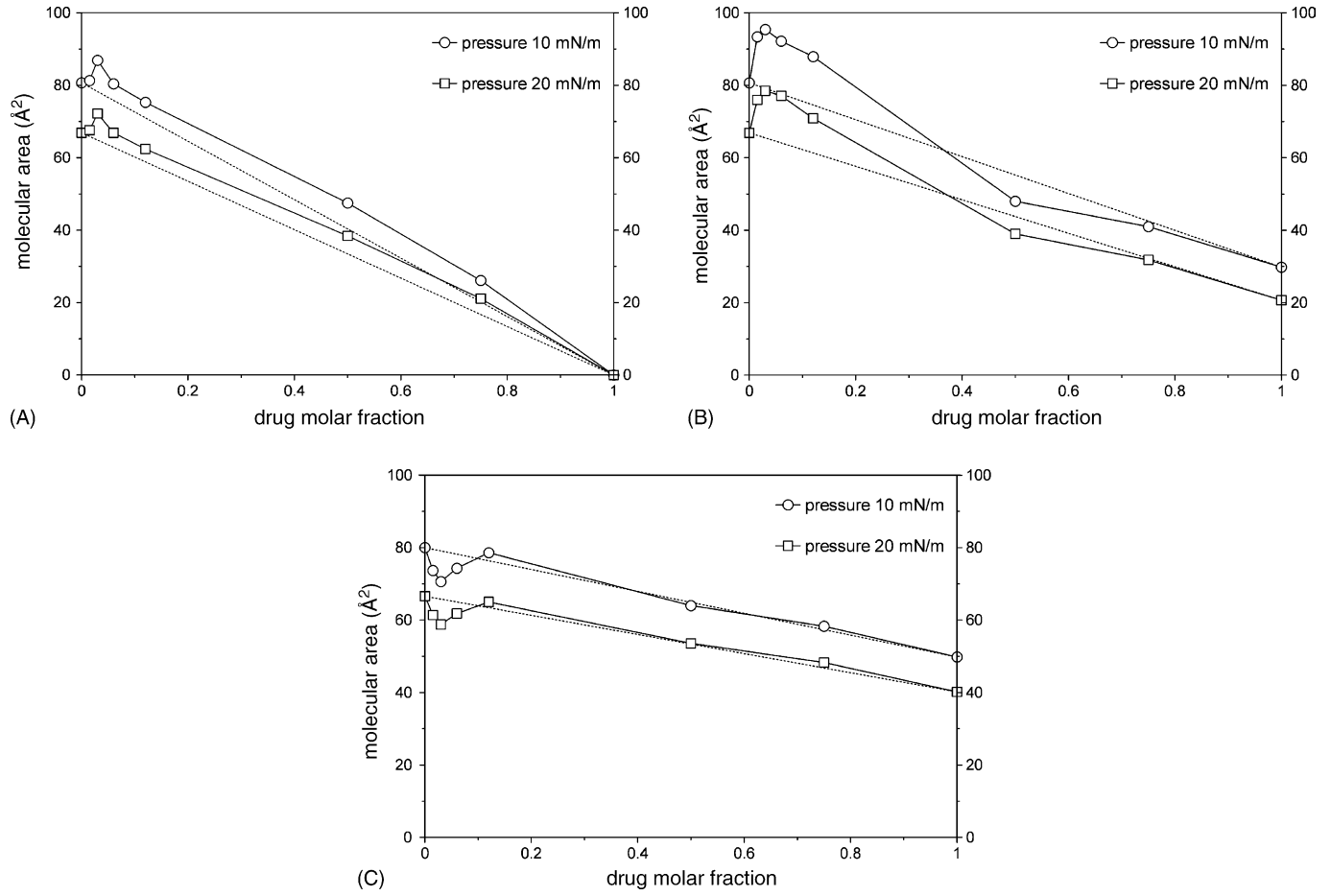

Fig. 12. Molecular area vs. **2a** (A), **4a** (B), and **6a** (C) molar fractions, at 37 °C, for pressures of 10 and 20 mN/m. The dotted lines correspond to the ideal DMPC/TCP–LAA interaction.

mixtures, at lower conjugate molar fractions, the hydrophobic interactions were weak, whereas at higher molar fractions hydrophobic interactions became stronger giving rise to a better miscibility. To explain this expanding effect, the molecules' lateral motions must be invoked. Of course, lateral motions of **2a** and **4a** were favored with respect to DMPC molecules, whose two acyl chains hinder this kind of movement. Conjugate **4a** exhibited a stronger effect as its molecules occupy a larger area.

The behavior of compound **6a** was quite different: its longer alkyl side chain increased the **6a**/DMPC hydrophobic interactions and then the miscibility with DMPC molecules or, in the case of complete immiscibility, DMPC/DMPC and **6a**/**6a** interactions will be favored. These results are in agreement, from a qualitative point of view, with those collected from the DSC experiments. In fact, similarly to the destabilizing behavior observed in DSC runs, the expanding effect of TCP–LAA conjugates on DMPC monolayer increased from **2a** to **4a**, thereafter diminishing for **6a**. By a first approximation, lipid bilayers are back to back lipid monolayers at surface pressures between 45 and 50 mN/m (Gaines, 1966; Hui et al., 1975). The different surface pressures applied to monolayers and bilayers can cause the quantitative differences observed in the two kinds of experiments.

3.4. Correlation with in vitro biological data

The MAO inhibitory activity of compounds **1a**–**7a** (expressed as pI_{50}) (Pignatello et al., 2005) was plotted versus the length of the alkyl side chain of the LAA moiety (Fig. 13). A much closer profile than that one registered for DSC data (cf. Fig. 3) was obtained. In the DSC experiments the intermediate terms of the

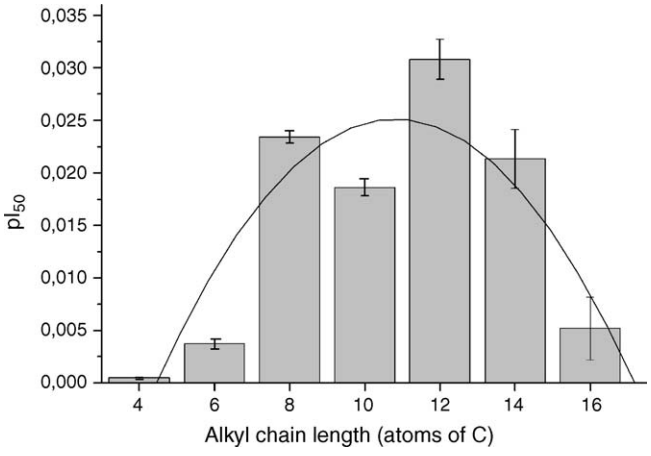

Fig. 13. Relationship between the lipophilicity and MAO inhibitory activity of compounds **1a**–**7a** (at the concentration of 100 μM).

series (from octyl to dodecyl derivative, **3a**–**5a**) were those able to interact more deeply and to a similar extent with the phospholipid bilayers and perturb their ordered packing, whereas the lower and higher homologues showed a reduced enzyme inhibitory activity and a poorer interaction with liposomes. A similar parabolic profile was obtained regarding the biochemical experiments (Fig. 13), with the intermediate members of the series **3a**–**6a** showing the best MAO inhibitory activity. Such a comparison was a further confirmation of the value of DSC studies in predicting the interaction of drugs with cells and biological structures.

4. Conclusions

Conjugation of TCP, a classical MAO inhibitor, with short, medium, and long-alkyl side chain LAA residues provided a set of molecular tools that could be useful to evaluate the effects of increasing lipophilicity/amphiphilicity on their interaction with biological membranes.

A battery of *wet and dry* methods with the in vitro assays as a conclusive hinge, seems to confirm the main aim of this study: LAA conjugation to drugs is able to merge lipophilicity and amphiphilicity, resulting in a broader interaction with phospholipid biomembrane models. Such deduction was corroborated by observing that the simple increase of lipophilicity induced by drug derivatization with alkanoic acid residues did not supply a similar membrane-like character to the corresponding TCP amides.

LAA have been proposed as promoieties able to impart a 'membrane-like character' to drug molecules (Toth, 1994). Our calorimetric and computational evidences support such hypothesis and the proposal of LAA – particularly those containing a medium to long side alkyl chain – as useful fragments to improve the biopharmaceutical profile and overall bioavailability of peptides and drugs.

Moreover, the structure–property relationships obtained from the calorimetric experiments of interaction with DMPC bilayers showed to fit well with the in vitro biological activity profile given by these MAOI agents.

Acknowledgements

This work was supported by the Italian Ministero dell'Istruzione e della Ricerca (MIUR) (PRIN2003 project: "Trasporto e rilascio di farmaci nel sistema nervoso centrale mediante coniugati lipidici e sistemi colloidali"). We are grateful to Dr. Manfred Kansy (Hoffmann-La Roche) for the Hoffmann-La Roche computational resources (Adapted Clark Method) in support of this work and his valuable discussion.

References

Albrecht, O., Gruler, H., Sackmann, E., 1978. Polymorphism of phospholipid monolayers. J. Phys. 39, 301–313.

Baláž, Š., 2000. Lipophilicity in trans-bilayer transport and subcellular pharmacokinetics. In: Martin, Y.C. (Ed.), Perspectives in Drug Discovery and Design. Hydrophobicity and Solvation in Drug design. Part III, vol. 19. Kluwer, Escom, Dordrecht, pp. 157–177.

Bodor, N., Buchwald, P., 2002. Barriers to remember: brain-targeting chemical delivery systems and Alzheimer's disease. Drug Today 7, 766–774.

Castelli, F., Raudino, A., Fresta, M., 2005. A mechanistic study of the permeation kinetics through biomembrane models: gemcitabine-phospholipid bilayer interaction. J. Colloid Interf. Sci. 285, 110–117.

Castelli, F., Librando, V., Sarpietro, M.G., 2002. Calorimetric approach of the interaction and absorption of polycyclic aromatic hydrocarbons with model membranes. Environ. Sci. Technol. 36, 2717–2723.

Clark, D.E., 2001. Prediction of intestinal absorption and blood–brain barrier penetration by computational methods. Comb. Chem. High Throughput Screen 4, 477–496.

Gaines, G.L., 1966. Insoluble Monolayers at Liquid–Gas Interfaces. Interscience, New York–London.

Grunewald, G.L., Pleiss, M.A., Catchell, C.L., Pazhenchevsky, R., Rafferty, M., 1984. Gas chromatographic quantitation of underivatized amines in the determination of their octanol–0.1 M sodium hydroxide partition coefficients by the shake-flask method. J. Chromatogr. 292, 319–331.

Hui, S.W., Cowden, M., Papahadjopoulos, D., Parsons, D.F., 1975. Electron diffraction study of hydrated phospholipid single bilayers. Effects of temperature hydration and surface pressure of the "precursor" monolayer. Biochim. Biophys. Acta 382, 265–275.

Jolliet-Riant, P., Tillement, J.P., 1999. Drug transfer across the blood–brain barrier and improvement of brain delivery. Fundam. Clin. Pharmacol. 13, 16–26.

Kaganer, V.M., Mohwald, H., Dutta, P., 1999. Structure and phase transitions in Langmuir monolayers. Rev. Modern Phys. 71, 779–819.

Pignatello, R., Jansen, G., Kathmann, I., Puglisi, G., Toth, I., 1998. Lipoamino acid conjugates of methotrexate with antitumor activity. J. Pharm. Sci. 87, 367–371.

Pignatello, R., Guccione, S., Forte, S., Di Giacomo, C., Sorrenti, V., Vicari, L., Uccello Barretta, G., Balzano, F., Puglisi, G., 2004. Lipophilic conjugates of methotrexate with short-chain alkylamino acids as DHFR inhibitors. Synthesis, biological evaluation, and molecular modelling. Bioorg. Med. Chem. 12, 2951–2964, and references cited therein.

Pignatello, R., Toth, I., Puglisi, G., 2001. Structural effects of lipophilic methotrexate conjugates on model phospholipid biomembranes. Thermochim. Acta 380, 255–264.

Pignatello, R., Puleo, A., Guccione, S., Raciti, G., Acquaviva, R., Campisi, A., Ventura, C.A., Puglisi, G., 2005. Enhancement of drug affinity for cell membranes by conjugation with lipoamino acids. I. Synthesis and biological evaluation of lipophilic conjugates of tranylcypromine. Eur. J. Med. Chem. 40, 1074–1079.

Plemper van Balen, G., Marca Martinet, C.A., Caron, G., Bouchard, G., Reist, M., Carrupt, P.-A., Fruttero, R., Gasco, A., Testa, B., 2004. Liposome/water lipophilicity: methods, information content, and pharmaceutical application. Med. Res. Rev. 24, 299–324.

Saija, A., Tomaino, A., Trombetta, D., Pellegrino, M.L., Tita, B., Caruso, S., Castelli, F., 2002. Interaction of melatonin with model membranes and possible implications in its photoprotective activity. Eur. J. Pharm. Biopharm. 53, 209–215.

Toth, I., 1994. A novel chemical approach to drug delivery: lipidic amino acid conjugates. J. Drug Target. 2, 217–239.

Waterhouse, R.N., 2003. Determination of lipophilicity and its use as a predictor of blood–brain barrier penetration of molecular imaging agents. Mol. Imaging Biol. 5, 376–389.

Wong, A., Toth, I., 2001. Lipid, sugar and liposaccharide based delivery systems. Curr. Med. Chem. 8, 1123–1136.